

H-Fac: Memory-Efficient Optimization with Factorized Hamiltonian Descent

Son Nguyen* Lizhang Chen Bo Liu Qiang Liu

The University of Texas at Austin
{sonnv77,lzchen,bliu,lqiang}@utexas.edu

Abstract

In this study, we introduce a novel adaptive optimizer, *H-Fac*, which incorporates a factorized approach to momentum and scaling parameters. Our algorithm demonstrates competitive performances on both ResNets and Vision Transformers, while achieving sublinear memory costs through the use of rank-1 parameterizations for moment estimators. We develop our algorithms based on principles derived from Hamiltonian dynamics, providing robust theoretical underpinnings. These optimization algorithms are designed to be both straightforward and adaptable, facilitating easy implementation in diverse settings.

1 Introduction

Optimization algorithms play an indisputable role in the remarkable development of AI, especially in the realm of modern deep learning. In recent years, the emergence of breakthroughs in architectural innovation [3], as well as practical applications [37], has further promoted the necessity for embracing efficient training paradigms, which encompass optimization algorithms striking a balance between performance and manageable memory costs.

Stochastic gradient descent (SGD) is widely regarded as the standard algorithm for training deep learning models, supported by extensive theoretical foundations [31, 32, 34, 43]. However, it requires thorough tuning of hyperparameters and frequently exhibits undesirable convergence rates when applied to many contemporary architectures [10, 36, 40]. Meanwhile, adaptive gradient methods such as Adam [17], AdaGrad [12], AMSGrad [29], etc., can adjust the learning rate for each parameter throughout the optimization process by utilizing cumulative second-order statistics. Although the theoretical aspects have not yet been fully exploited, these methods show empirical performance that surpasses SGD across multiple domains and often provides better convergence properties in practice [41, 24], making them highly appealing for large-scale applications. However, maintaining momentum and per-coordinate scaling parameter accumulators in these algorithms will significantly increase memory overhead. This barrier typically restricts model size, reduces the number of examples per mini-batch, or limits communication in decentralized training [18, 21, 22], thereby negatively affecting convergence and accuracy.

Several memory-efficient optimizers have been devised to address this problem. In particular, Adafactor [30] is a highly efficient algorithm that was designed for low memory usage and greater scalability. It achieves substantial memory savings by employing the non-negative matrix factorization approach [19] to decompose the second-moment accumulator into two distinct rank-1 factors. This technique not only minimizes memory footprint but also enhances computational efficiency. However, to avoid performance degradation, Adafactor still needs to maintain first-order

*Correspondence to Son Nguyen: sonnv77@utexas.edu

statistics, particularly when applied to large-scale models. This could potentially limit its applicability in memory-constrained environments. One of our goals is to address this inherent issue. Moreover, Adafactor does not yet have a solid theoretical foundation, which leaves its underlying methodologies and effectiveness without formal justification.

In this paper, we propose to approach the aforementioned open problems through the lens of Hamiltonian dynamics. Motivated by some inspirational works [4, 26], we explore how Hamiltonian principles in modeling dynamic systems can inform and improve optimization strategies, especially for memory efficiency purpose. Our contributions can be summarized in the following:

- We demonstrate that Adafactor can be deduced from an ordinary differential equation (ODE) that solves a minimization problem with constrained factors. This novel perspective allows us to derive other algorithms with the same principles.
- We propose a new class of efficient optimization algorithms that embraces both first-order and adaptive methods. By employing rank-1 parameterization for momentum and scaling parameter, our optimizers can offer sublinear memory costs, comparable to that of vanilla SGD without momentum. To the best of our knowledge, our proposal is the first endeavor to exploit Hamiltonian dynamics in developing a class of memory-efficient optimization algorithms that utilize factorized gradient statistic estimators.
- Distinct from existing optimization techniques for memory efficiency, our algorithm can offer clear insights into optimization dynamics and convergence guarantees, which are naturally inherited from the fundamental theory of Hamiltonian mechanics.
- Empirical results show that our optimization algorithms can achieve favorable and comparable results on ResNets and Vision Transformers.

Organization. The rest of the paper is organized as follows. The next section will discuss related works on memory-efficient optimization. We will provide in section 3 a brief overview of the Hamiltonian descent framework. Section 4 presents our main methodological contributions. The experimental results are shown in section 5. Finally, in section 6, we will discuss the current limitations, as well as the potential of our proposal for future works. The proofs and some other results are left in Appendix.

Notations: We denote model parameters by a matrix X of size $m \times n$. Let $\mathbf{1}_m$ and $\mathbf{1}_n$ be vectors of ones with dimensions m and n , respectively. For any matrices X, Y of size $m \times n$, we use \sqrt{X} for element-wise square root, X^2 for element-wise square, and X/Y to denote element-wise division. X^\top stands for the transpose matrix, $\text{trace}(X)$ denotes the trace of matrix X , and the function $\text{RMS}(X) = \sqrt{\frac{1}{m \times n} \sum_{i,j} X_{ij}^2}$ represents root-mean-square calculation.

2 Related Works

In this section, we provide a brief overview of existing memory-efficient optimization methods.

Developing memory-efficient optimization algorithms is increasingly critical and attempts to minimize memory usage of optimizers are based on many different aspects. Adafactor [30] minimizes the memory cost to a sublinear level by factorizing second-order statistics using a row-column outer product. Luo et al. [25] introduced a confidence-guided strategy to mitigate erroneous updates and reduce instability in Adafactor training, while still retaining the same memory footprint. SM3 [1]

is another efficient algorithm, which organizes the parameter space into sets and simplifies the maintenance of second-order statistics by computing the maximum squared gradient for each set.

There are several methods that focus on the low-rank structure of the gradient rather than the moment statistics [15, 42]. For instance, GaLore [42] periodically applies Singular Value Decomposition (SVD) to project the full gradients onto a lower-dimensional subspace, and subsequently utilize these projected gradients in adaptive optimization processes. Sketchy [13] leverages the Frequent Directions (FD) sketch technique to maintain a low-rank approximation of the gradient covariances matrix. Additionally, there is a line of work adapting quantization to reduce the memory cost of optimizer states [8, 9, 20].

For second-order (Hessian-based) methods, the memory constraints primarily arise from computing the (inverse) Hessian matrix. Some successful works have also resolved this bottleneck using Gauss-Newton decomposition [23] or Kronecker-based factorization [27].

3 Background

3.1 Hamiltonian Descent

We consider an unconstrained, continuous optimization problem $\min_{X \in \mathbb{R}^{m \times n}} f(X)$, with a proper differentiable and lower bounded objective $f : \mathbb{R}^{m \times n} \rightarrow \mathbb{R}$. In deep learning particularly, gradient-based optimization algorithms have been the de facto choice for solving such problems. Gradient descent with momentum (GDm) is one widely adopted such method due to its simplicity and effectiveness. Specifically, the update procedure of GDm is based on the following iterative scheme:

$$M_t = \beta M_{t-1} + \nabla f(X_{t-1}), \quad X_t = X_{t-1} - \eta_t M_t,$$

where η_t is the step size at the t -th iteration, $\beta \in (0, 1)$ is a coefficient controlling how much we decay the old momentum at each step. In case we employ *full-batch* gradients, this scheme is deterministic and can be viewed as a discretization of a *continuous-time system* [26, 14] as follows

$$\dot{M} = -\gamma M - \nabla f(X), \quad \dot{X} = M, \tag{1}$$

where M and γ are in analogy to the *velocity* the *friction* in classical mechanics. In principle, this ordinary differential equation (ODE) defines a trajectory of the particle X_t and its velocity M_t , which drives the systems characterized by the *total energy* or Hamiltonian function,

$$H(X, M) = f(X) + \|M\|_2^2/2,$$

towards stationary points. Indeed, we can show that the Hamiltonian H_t is monotonically decreasing along the ODE trajectory:

$$\frac{d}{dt} H = \text{trace}(\nabla^\top f(X) \dot{X}) + \text{trace}(M^\top \dot{M}) = -\gamma \text{trace}(M^\top M) = -\gamma \|M\|_F^2 \leq 0.$$

in which $\|\cdot\|_F$ is the Frobenius norm. This interpretation is meaningful in the sense that it facilitates us to theoretically establish a broader class of optimizers with guarantees, as well as providing complementary insights, improving or extending existing algorithms. In the next section, we will strengthen this argument by extending the Hamiltonian framework to more modern algorithms, and especially provide new memory-efficient optimizers based on this principle.

Algorithm 1 Adafactor-m for matrix parameter, with factored second moments and first-moment decay coefficient β_1 .

Inputs: moment decay coefficients β_1, β_2 , smoothing term ϵ , and regularization constant λ

Initialization: weight parameters $X_0 \in \mathbb{R}^{m \times n}$, initial moments $M_0, r_0, s_0 \leftarrow 0$

for $t = 1$ to T **do**

$$G_t = \nabla f_t(X_{t-1})$$

$$M_t = \hat{\beta}_{1t} M_{t-1} + (1 - \hat{\beta}_{1t}) G_t$$

$$r_t = \hat{\beta}_{2t} r_{t-1} + (1 - \hat{\beta}_{2t}) [(G_t)^2 + \epsilon] \mathbf{1}_n$$

$$s_t = \hat{\beta}_{2t} s_{t-1} + (1 - \hat{\beta}_{2t}) [(G_t^\top)^2 + \epsilon] \mathbf{1}_m$$

$$\hat{V}_t = r_t s_t^\top / (\mathbf{1}_m^\top r_t)$$

$$X_t = X_{t-1} - \eta_t \left(\text{clip} \left(M_t / \sqrt{\hat{V}_t} \right) + \lambda X_{t-1} \right)$$

end for

4 Factorized Hamiltonian Descent

In this section, we first interpret Adafactor optimizer from the perspective of Hamiltonian descent. We then introduce a general method to factorize the momentum in first-order optimization methods. We will specifically deliver a factorization version for the sign-based momentum update and name this optimizer as *signFSGD*. Based on further insights, we propose a novel adaptive factorized optimization method, named *H-Fac*. This is our main algorithm contribution to this paper.

4.1 Adafactor optimizer as Hamiltonian

Adafactor [30] shown in Algorithm 1 proposed an efficient rank-1 parameterization for the scaling factor, $V = r s^\top$, which is widely employed in adaptive optimization methods like Adam [17], RMSprop [35], etc. The updates of vectors r and s were inspired by the total elementwise I-divergence subject to componentwise non-negative constraints:

$$\underset{r \in \mathbb{R}^m, s \in \mathbb{R}^n}{\text{minimize}} \sum_{i=1}^m \sum_{j=1}^n d(V_{ij}, r_i s_j),$$

in which $r_i \geq 0, s_j \geq 0$ and $d(p, q) = p \log \frac{p}{q} - p + q$.

Solving this problem results in a closed-form solution denoted by $r = V \mathbf{1}_m, s = V^\top \mathbf{1}_n / r^\top \mathbf{1}_m$. Subsequently, the iterative process of Adafactor optimizer can be outlined as in Algorithm 1, in which the decay parameter $\hat{\beta}_{2t} = \beta_2(1 - \beta_2^{t-1}) / (1 - \beta_2^t)$ is defined as equivalent to the bias correction step. In the model parameter update, we have $\text{clip}(U) = U / \max(1, \text{RMS}(U)/d)$ with $\text{RMS}(\cdot)$ refers to the root-mean-square function and d is the threshold value, meaning that we cap the norm of the actual update rather than just the gradient. This technique aims to eliminate the larger-than-desired updates and also stabilize the training process with slow decay ($\beta_2 = 0.999$).

Briefly, Adafactor tracks the moving averages of the row and column sums of squared gradients throughout iterations, resulting in factored second-moment estimators r_t and s_t . A normalized outer product $r_t s_t^\top / (\mathbf{1}_m^\top r_t)$ is then used to reconstruct a low-rank parameterization of second-order momentum. This technique is computationally efficient and scalable as it offers analytical formulations without the need for additional approximations. However, directly applying a non-negative decomposition approach like that often appears heuristic. It fails to provide any insights

into the optimization dynamics and convergence guarantees when we reparameterize the second-order statistic using such a low-rank representation. Interestingly, we demonstrate that the iterative procedure in Adafactor-m optimizer can be discretized from an ordinary differential equation (ODE) as follows:

$$\dot{X} = -\frac{M}{\sqrt{rs^\top/1_m^\top r}}, \quad \dot{M} = \nabla f(X) - \alpha M, \quad \dot{r} = (\nabla f(x))^2 1_n - \alpha r, \quad \dot{s} = (\nabla^\top f(x))^2 1_m - \alpha s$$

// Adafactor-m (ODE)

which solves a minimization problem with respect to the Hamiltonian function described by:

$$H(X, M, r, s) = f(X) + \frac{1}{2} \sum_{i=1, j=1}^{m, n} \frac{M_{ij}^2 \sqrt{\sum_{i=1}^m r_i}}{\sqrt{r_i s_j}}.$$

Proposition 1. *A key property is that the function H monotonically decreases along the ODE trajectory, that is, $\frac{d}{dt}H(X_t, M_t, r_t, s_t) \leq 0$.*

A detailed proof is provided in Appendix A.2.

By formulating the update scheme as an ODE, we can elaborate on the dynamics of the optimization process, and more importantly, it facilitates theoretical insights into the stability and convergence properties. In the next sections, we will broaden this perspective to encompass a wider range of optimizers, including first-order and adaptive algorithms. By doing so, we aim to integrate various optimization techniques within a unified framework of Hamiltonian dynamics.

4.2 Factorized first-order momentum estimation

Factoring the second-order momentum is a straightforward yet intuitive idea to handle memory overhead. This approach offers an advantage in that it allows for the tolerance of information loss, as our focus is solely on the magnitude of the scaling parameter. On the other hand, an inherent drawback of most algorithms is the need to maintain a full momentum to avoid performance degradation. However, dealing with first-order information poses more challenging problems because we must consider both the magnitude and especially the update directions.

Factorization via rank-1 parameterization. We propose here a sublinear memory optimizer that factorizes the first-order momentum. The algorithm is specifically derived from an ordinary differential equation outlined as follows (recall that $X \in \mathbb{R}^{m \times n}$ is a matrix):

$$\begin{aligned} \dot{X} &= -\nabla\phi(\beta\hat{u}1_n^\top + \nabla f(X)) - \nabla\psi(\beta1_m\hat{v}^\top + \nabla f(X)) \\ \dot{u} &= \nabla f(X)1_n/n - \alpha u, & \hat{u} &= u - \nabla f(X)1_n/n \\ \dot{v} &= \nabla^\top f(X)1_m/m - \alpha v, & \hat{v} &= v - \nabla^\top f(X)1_m/m. \end{aligned} \tag{2}$$

where α, β are two positive parameters; ϕ and ψ are any convex functions, such that $\nabla\phi(\cdot), \nabla\psi(\cdot)$ are monotonic operators. The simplest option to consider is that $\phi(X) = \psi(X) = \|X\|_2^2/2$, then their gradients $\nabla\phi(X) = \nabla\psi(X) = X$. This system yields the Hamiltonian function:

$$H(X, u, v) = f(X) + \frac{\beta n}{2} \|u\|_2^2 + \frac{\beta m}{2} \|v\|_2^2.$$

A detailed analysis of this function is provided in Appendix A.1.

Algorithm 2 *signFSGD* for matrix parameter, with factored first-order moments.

Inputs: moment coefficients $\beta = 0.9$, and regularization constant λ

Initialization: weight parameters $X_0 \in \mathbb{R}^{m \times n}$, initial moment factors $u_0, v_0 \leftarrow 0$

for $t = 1$ to T **do**

$$G_t = \nabla f_t(X_{t-1})$$

$$u_t = \beta u_{t-1} + (1 - \beta)G_t \mathbf{1}_n / n$$

$$v_t = \beta v_{t-1} + (1 - \beta)G_t^\top \mathbf{1}_m / m$$

$$\hat{u}_t = u_t - G_t \mathbf{1}_n / n$$

$$\hat{v}_t = v_t - G_t^\top \mathbf{1}_m / m$$

$$X_t = X_{t-1} - \eta_t \left(\text{sign} \left(\beta \hat{u}_t \mathbf{1}_n^\top + G_t \right) + \text{sign} \left(\beta \mathbf{1}_m \hat{v}_t^\top + G_t \right) + \lambda X_{t-1} \right)$$

end for

Back to our framework, a number of remarks are in order:

1) Compared with algorithms that maintain a full rank momentum matrix $M \in \mathbb{R}^{m \times n}$ in like equation 1, this algorithm employs two rank-one momentum vectors $u \in \mathbb{R}^m$ and $v \in \mathbb{R}^n$, which significantly reduces the memory cost from $O(mn)$ to $O(m + n)$. In the algorithm, we use the simple unit vectors $\mathbf{1}_m, \mathbf{1}_n$ to first down project the full gradient $\nabla f(X)$ into the rank-one spaces of column means and row means, and exponentially accumulate these statistics across training steps. We then reconstruct the rank-one momentum \hat{u}, \hat{v} to update the model parameters. The \hat{u} and \hat{v} are centralized variants of u and v .

2) Discretizing ODE equation 2 using the Euler method results in the following iterative scheme:

$$\begin{aligned} u_t &= \hat{\beta}_{1t} u_{t-1} + (1 - \hat{\beta}_{1t}) \nabla f(X_t) \mathbf{1}_n / n, & \hat{u}_t &= u_t - \nabla f(X_t) \mathbf{1}_n / n \\ v_t &= \hat{\beta}_{1t} v_{t-1} + (1 - \hat{\beta}_{1t}) \nabla^\top f(X_t) \mathbf{1}_m / m, & \hat{v}_t &= v_t - \nabla^\top f(X_t) \mathbf{1}_m / m \\ X_t &= X_{t-1} - \eta_t \left[\nabla \phi \left(\hat{\beta}_{1t} \hat{u}_t \mathbf{1}_n^\top + \nabla f(X_t) \right) + \nabla \psi \left(\hat{\beta}_{1t} \mathbf{1}_m \hat{v}_t^\top + \nabla f(X_t) \right) \right] \end{aligned}$$

In discrete-time analysis, we centralize the row means and column means statistics u_t, v_t by corrected terms $\nabla f(X_t) \mathbf{1}_n / n$ and $\nabla^\top f(X_t) \mathbf{1}_m / m$, respectively. These corrected terms are essential as they can guarantee the updates inside $\nabla \phi(\cdot)$ and $\nabla \psi(\cdot)$ will converge to the true first moment $\mathbb{E}[\nabla f(X_t)]$. Specifically, by unfolding the factored moment u_t (similarly to v_t), we can get an accumulator of column-wise mean of gradients in the form:

$$u_t = \sum_{i=1}^t (1 - \hat{\beta}_{1i}) \prod_{j=i+1}^t \hat{\beta}_{1j} \nabla f(X_i) \mathbf{1}_n.$$

By the assumption that the gradient distribution is stationary, taking expectations gives us:

$$\mathbb{E}[u_t] = \sum_{i=1}^t (1 - \hat{\beta}_{1i}) \prod_{j=i+1}^t \hat{\beta}_{1j} \mathbb{E}[\nabla f(X_i) \mathbf{1}_n] = \sum_{i=1}^t (1 - \hat{\beta}_{1i}) \prod_{j=i+1}^t \hat{\beta}_{1j} \mathbb{E}[\nabla f(X_t) \mathbf{1}_n].$$

Futhermore, we can prove by induction that $\sum_{i=1}^t (1 - \hat{\beta}_{1i}) \prod_{j=i+1}^t \hat{\beta}_{1j} = 1$, leading to $\mathbb{E}[u_t] = \mathbb{E}[\nabla f(X_t) \mathbf{1}_n]$ and hence the expected value of centralized moment factor $\mathbb{E}[\hat{u}_t]$ will approximate the true first-order moment $\mathbb{E}[\nabla f(X_t)]$.

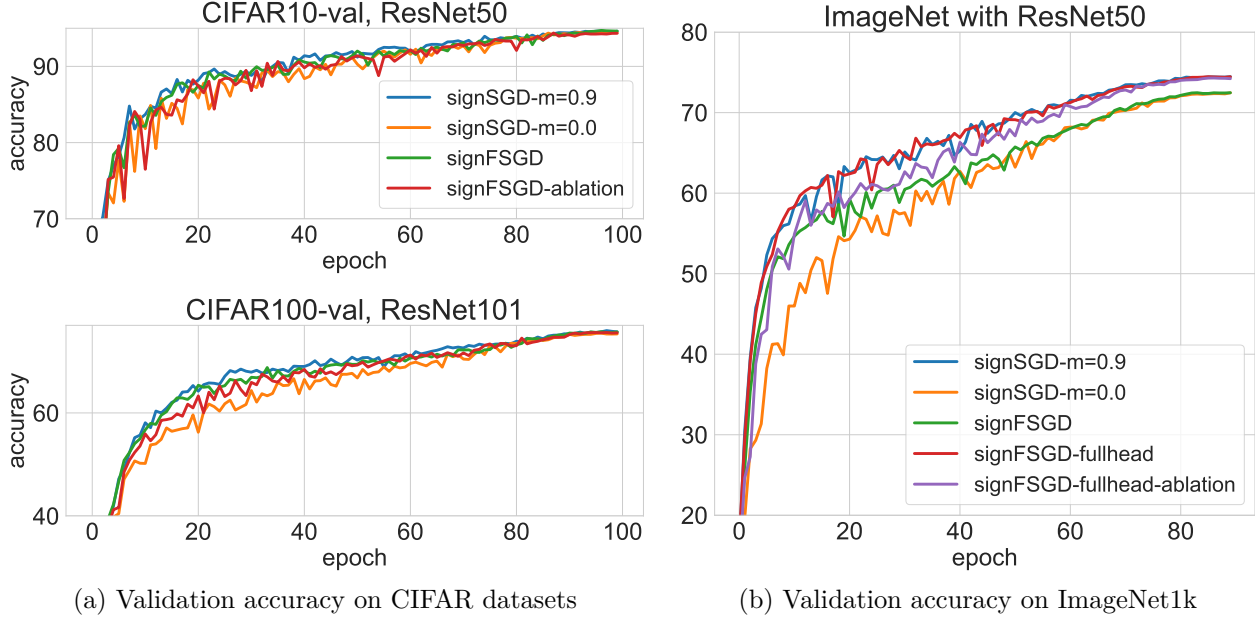


Figure 1: A comparison of optimizer performance on ResNet architectures. For *signSGD*, m denotes the momentum coefficient. For *signFSDG*, “*ablation*” means the version without corrected terms, “*fullhead*” means the version using full momentum for the MLP head layer.

3) When the momentum coefficient is deactivated ($\beta_1 = 0$), the update terms inside $\nabla\phi(\cdot)$ and $\nabla\psi(\cdot)$ degenerate to $\nabla f(X_t)$. In this scenario, the algorithm simplifies to standard gradient descent:

$$\dot{X} = -\nabla\phi(\nabla f(X)) - \nabla\psi(\nabla f(X)).$$

To empirically examine the prospects of our general framework and especially the necessity of the corrected terms, we conducted a basic image classification experiment on the CIFAR10 and CIFAR100 datasets using ResNet50 and ResNet101, respectively. We choose $\phi(\cdot)$ and $\psi(\cdot)$ to be the L_1 -norm, namely $\phi(X) = \psi(X) = \|X\|_1$, resulting in their gradients $\nabla\phi(\cdot)$ and $\nabla\psi(\cdot)$ being the *sign*(\cdot) functions. In this case, we refer to our algorithm as *signFSGD 2*, which incorporates a rank-1 parameterization to factorize the momentum in *signSGD* optimizer [2]. We will evaluate the effectiveness of *signFSGD* with and without the corrected terms and compare its performance to that of *signSGD* with momentum enabled or disabled. Figure 1a shows that *signFSGD* can yield comparable results to *signSGD* with momentum. However, without the corrected terms, our algorithm is generally less stable and only gains relative improvements compared to *signSGD* without momentum. Thus, simply accumulating row means and column means of gradient information across training steps is insufficient to accelerate the optimization process.

Motivated by the recent development of Lion optimizer [6], we adopted an efficient technique called double- β scheme to further improve the performance of *signFSGD* on ResNet models. We refer to this new algorithm as *LionFactor 4*, and provide some discussions in Appendix B.

4.3 Fully factorized momentum estimations

Inadequacy of first-order factorization. For ResNet models, mini-batch gradients are typically quite small and well concentrated around zero mean as shown in Figure 2. Consequently, accu-

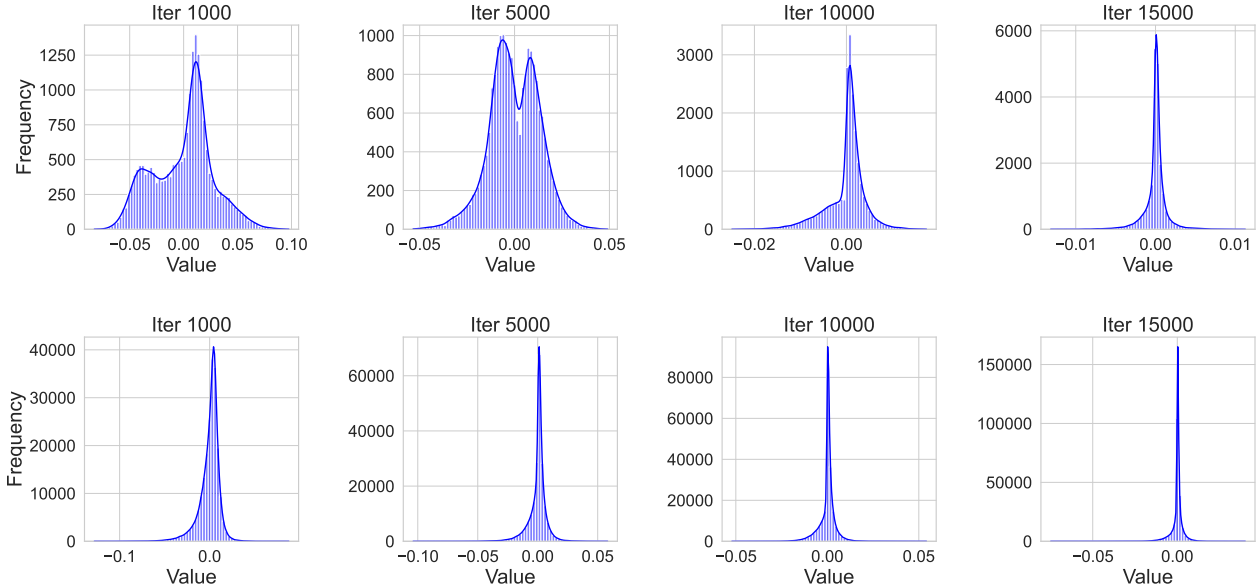


Figure 2: Histograms illustrating the gradients of MLP head layers in ResNet50 (top) and ResNet101 (bottom) trained on CIFAR10 and CIFAR100, respectively.

mutating the momentum through column means and row means of the gradient information will significantly flatten the magnitude. This issue could potentially reduce the impact of momentum on the optimization updates, especially with large-scale settings such as ImageNet and modern deep learning architectures.

In Figure 1b, we present the performances of *signSGD* and *signFSGD* when training ResNet50 from scratch on ImageNet1k. Notably, our method does not yield substantial enhancements compared to *signSGD* without momentum as observed on CIFAR10, CIFAR100 datasets. However, when employing a full momentum instead of the factorized one for the MLP head layer, our *signFSGD* can perform comparably to *signSGD* with momentum. We witness the same behavior when applying the algorithm to larger ResNet architectures.

This observation reinforces our previous remark regarding the moderate impact of our factorized first-order momentum on scale models. Although a few minor customizations, such as omitting the factorization of the MLP head layer like above, could overcome the issue on ResNets, our initial expectation leaned towards a more general-purpose optimization algorithm. We specifically aim to extend the scalability of our algorithms to encompass modern convolution-free architectures, such as Vision Transformers.

Incorporating second-order information. A natural idea to deal with the magnitude issue of factorized first-order momentum is to normalize them by factored second moments. Indeed, by integrating our factorization for the first moment estimator into Adafactor, we can establish a unified method where both momentum estimators are fully factorized. In principle, we aim to conceptualize our algorithms within Hamiltonian frameworks, but deriving an objective function for such a simplistic integration might be challenging. We instead come up with a novel algorithm

Algorithm 3 *H-Fac* for matrix parameters, with both first and second-order moments factorized.

Inputs: moment decay coefficients β_1, β_2 , smoothing term ϵ , and regularization constant λ

Initialization: weight parameters $X_0 \in \mathbb{R}^{m \times n}$, initial factored moments $u_0, v_0, r_0, s_0 \leftarrow 0$

for $t = 1$ to T **do**

$$G_t = \nabla f_t(X_{t-1})$$

$$u_t = \hat{\beta}_{1t} u_{t-1} + (1 - \hat{\beta}_{1t}) G_t \mathbf{1}_n / n$$

$$v_t = \hat{\beta}_{1t} v_{t-1} + (1 - \hat{\beta}_{1t}) G_t^\top \mathbf{1}_m / m$$

$$r_t = \hat{\beta}_{2t} r_{t-1} + (1 - \hat{\beta}_{2t}) [(G_t)^2 + \epsilon] \mathbf{1}_n$$

$$s_t = \hat{\beta}_{2t} s_{t-1} + (1 - \hat{\beta}_{2t}) [(G_t^\top)^2 + \epsilon] \mathbf{1}_m$$

$$\hat{V}_t = r_t s_t^\top / (\mathbf{1}_m^\top r_t)$$

$$\phi_{term} = \hat{\beta}_{1t} (u_t \mathbf{1}_n^\top - G_t \mathbf{1}_n \mathbf{1}_n^\top / n) / \sqrt{r_t \mathbf{1}_n^\top / n}$$

$$\psi_{term} = \hat{\beta}_{1t} (\mathbf{1}_m v_t^\top - \mathbf{1}_m \mathbf{1}_m^\top G_t / m) / \sqrt{\mathbf{1}_m s_t^\top / m}$$

$$X_t = X_{t-1} - \eta_t \left(0.5 (\phi_{term} + \psi_{term}) + \text{clip} \left(G_t / \sqrt{\hat{V}_t} \right) + \lambda X_{t-1} \right)$$

end for

characterized by the following ODE:

$$\dot{X} = -\frac{1}{2} \left(\frac{u \mathbf{1}_n^\top - \nabla f(X) \mathbf{1}_n \mathbf{1}_n^\top / n}{\sqrt{r \mathbf{1}_n^\top}} + \frac{\mathbf{1}_m v^\top - \mathbf{1}_m \mathbf{1}_m^\top \nabla f(X) / m}{\sqrt{\mathbf{1}_m s^\top}} \right) - \frac{\nabla f(X)}{\sqrt{r s^\top / \mathbf{1}_m^\top r}}$$

$$\dot{u} = \nabla f(X) \mathbf{1}_n / n - \alpha u$$

$$\dot{v} = \nabla^\top f(X) \mathbf{1}_m / m - \alpha v$$

$$\dot{r} = (\nabla f(X))^2 \mathbf{1}_n - \alpha r$$

$$\dot{s} = (\nabla^\top f(X))^2 \mathbf{1}_m - \alpha s$$

// *H-Fac* (ODE)

which yields the following Hamiltonian function:

$$H(X, u, v, r, s) := f(X) + \frac{n}{4} \sum_{i=1}^m \frac{u_i^2}{\sqrt{r_i}} + \frac{m}{4} \sum_{j=1}^n \frac{v_j^2}{\sqrt{s_j}}.$$

Proposition 2. *The function H monotonically decreases along the ODE trajectory.*

A detailed proof is provided in Appendix A.3.

The discrete-time equivalent is presented in Algorithm 3. In fact, this algorithm is inspired by a variant of AdamW optimizer outlined in Appendix C. Our model parameters update can be seen as an accumulator of normalized gradients, where both the momentum and the current gradient are normalized by their corresponding cumulative second-moment information. More specifically, our update includes a combination of three key elements: (1) the normalized momentum factorization $0.5 * (\phi_{term} + \psi_{term})$, in which the factorized first-order moment in section 4.2 is normalized by the row means and the column means of second-moment estimators; (2) a clipping of normalized gradient $\text{clip}(G_t / \sqrt{\hat{V}_t})$ which is inherited from Adafactor update; and (3) a decouple weight decay λX_{t-1} for enhancing the generalization performance of adaptive optimizers [24].

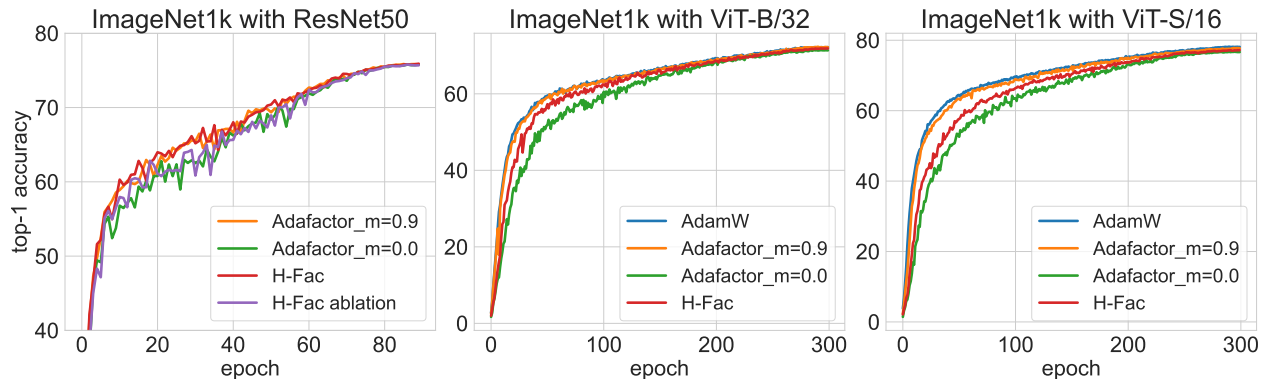


Figure 3: Top-1 Accuracy of optimizers in training ResNet50, ViT-B/32, and ViT-S/16 from scratch on the ImageNet1k. For *H-Fac*, “ablation” means the version without corrected terms.

Table 1: ImageNet1k top-1 accuracy results for various optimizers on different models.

Optimizers	<i>signSGD</i>		<i>signFSGD</i>	<i>signFSGD</i>	AdamW	Adafactor		<i>H-Fac</i>
	<i>m</i> = 0.9	<i>m</i> = 0.0		<i>-fullhead</i>		<i>m</i> = 0.9	<i>m</i> = 0.0	
ResNet50	74.47	72.36	72.47	74.45	75.66	75.85	75.79	75.90
ViT-B/32					72.20	72.31	71.36	71.87
ViT-S/16					78.16	77.81	76.74	77.20

5 Experiments

In this section, we conduct several experiments to demonstrate the effectiveness of our *H-Fac* algorithm. Unlike the earlier proposal of *signFSGD*, we do not customize the algorithm for any specific layers, but perform factorization on the entire architectures.

Experimental Setup We evaluated the optimization algorithms described in this paper mainly on the image classification task, specifically training ResNet50 and Vision Transformers from scratch on ImageNet1k, following previous works [11, 16]. The images are pre-processed by Inception-style cropping [33] and random horizontal. We train ResNet50 for 90 epochs, using a batch size of 1024, with cosine learning rate decay scheduler. For Vision Transformers (ViTs), we train them for 300 epochs, using a batch size of 4096, with a learning rate schedule of 10,000 steps warmup followed by linear decay. We also adopted strong data augmentations, including RandAugment(2,15) [7] and mixup (0.5) [39], to boost ViTs performances. We opted for recommended configurations from prior research for hyperparameters such as learning rate (*lr*) and weight decay (λ), dropout (*dr*):

- $lr = 3e - 4$, $\lambda = 1.0$ in sign-based optimizers, $lr = 1e - 3$, $\lambda = 0.1$ in adaptive algorithms when training ResNet50 on ImageNet.
- $lr = 3e - 3$, $\lambda = 0.1$, $dr = 0$ in adaptive algorithms for training ViT-B/32, ViT-S/16 on ImageNet with strong augmentations.

5.1 Empirical Results

The results are shown in Figure 3 and Table 1. On ResNet50, we can notice consistent patterns with those in Figure 1b. While our algorithm, *H-Fac*, can achieve similar memory efficiency as Adafactor without momentum, it demonstrates more stable training and delivers highly competitive performance compared to Adafactor with momentum. A performance degradation is also clearly observed in the ablation version, consolidating the significance of the corrected terms in our algorithms. On ViT models, although our *H-Fac* can catch up AdamW and Adafactor with momentum, there are noticeable performance gaps between optimizers, especially during the early training stages. A positive sign is that the factorized momentum in our algorithm can actually accelerate the optimization process, as evidenced by significant improvements compared to Adafactor without momentum. It should be noted that our *signFSGD* algorithm does not perform well on ViT architectures, even when full momentum is applied to the head layer. This result is anticipated according to the inadequacies discussed in Section 4.3.

We can elaborate on these behaviors by exploring the trainability of ResNets and ViTs. Convolution-free architectures like ViTs and MLP-Mixer are theoretically more difficult to train, as highlighted by analyses of the neural tangent kernel (NTK) condition number [5, 38]. Additionally, Park et al. [28] further discovered through Hessian spectrum analysis that ResNets possess a locally convex loss landscape, while ViTs exhibit many directions corresponding to negative Hessian eigenvalues. These aspects imply the need for better-adapted momentum in optimizing convolution-free networks, and partially explain the varied effects of our factorized momentum on the architectures. It also makes sense to expect that leveraging new architectural innovations or methods for smoothing the loss landscape could improve our optimization algorithms.

6 Limitation and Discussion

We conducted a few large-scale experiments on language models (LLMs) but unfortunately, we found our factorized optimizers might not be very effective. In the sense that our *H-Fac* optimizer only gains negligible improvement compared to Adafactor without momentum. As the model size increases considerably, the rank-1 parameterization in our factorized momentum only offers very marginal contributions, which is insufficient to accelerate the optimization process as effectively as proper momentum. This suggests that developing algorithms with rank- k approximation, based on the same principles of Hamiltonian dynamics, can hold significant potential for future works.

In conclusion, our work in this paper represents one of the first attempts to unify and devise new adaptive optimization methods that are theoretically grounded in Hamiltonian frameworks. It would be exciting to see future research pursuing this direction to enhance understanding of existing algorithms and propose more efficient ones. For practical use, our current optimizers show promise in applications where ResNets are advantageous because of their efficient training nature. For example, we can adapt our algorithms to the federated learning optimization problem, so that the factored moment estimators can be efficiently communicated to accelerate the convergence. Other applications would also be of interest.

References

- [1] Rohan Anil, Vineet Gupta, Tomer Koren, and Yoram Singer. Memory efficient adaptive optimization. *Advances in Neural Information Processing Systems*, 32, 2019.
- [2] Jeremy Bernstein, Yu-Xiang Wang, Kamyar Azizzadenesheli, and Animashree Anandkumar. signsgd: Compressed optimisation for non-convex problems. In *International Conference on Machine Learning*, pages 560–569. PMLR, 2018.
- [3] Rishi Bommasani, Drew A Hudson, Ehsan Adeli, Russ Altman, Simran Arora, Sydney von Arx, Michael S Bernstein, Jeannette Bohg, Antoine Bosselut, Emma Brunskill, et al. On the opportunities and risks of foundation models. *arXiv preprint arXiv:2108.07258*, 2021.
- [4] Lizhang Chen, Bo Liu, Kaizhao Liang, and Qiang Liu. Lion secretly solves constrained optimization: As lyapunov predicts. *arXiv preprint arXiv:2310.05898*, 2023.
- [5] Xiangning Chen, Cho-Jui Hsieh, and Boqing Gong. When vision transformers outperform resnets without pre-training or strong data augmentations. *arXiv preprint arXiv:2106.01548*, 2021.
- [6] Xiangning Chen, Chen Liang, Da Huang, Esteban Real, Kaiyuan Wang, Hieu Pham, Xuanyi Dong, Thang Luong, Cho-Jui Hsieh, Yifeng Lu, et al. Symbolic discovery of optimization algorithms. *Advances in Neural Information Processing Systems*, 36, 2024.
- [7] Ekin Dogus Cubuk, Barret Zoph, Jonathon Shlens, and Quoc V. Le. Randaugment: Practical automated data augmentation with a reduced search space. *2020 IEEE/CVF Conference on Computer Vision and Pattern Recognition Workshops (CVPRW)*, pages 3008–3017, 2019.
- [8] Tim Dettmers, Mike Lewis, Sam Shleifer, and Luke Zettlemoyer. 8-bit optimizers via block-wise quantization. *arXiv preprint arXiv:2110.02861*, 2021.
- [9] Tim Dettmers, Artidoro Pagnoni, Ari Holtzman, and Luke Zettlemoyer. Qlora: Efficient finetuning of quantized llms. *Advances in Neural Information Processing Systems*, 36, 2024.
- [10] Jacob Devlin, Ming-Wei Chang, Kenton Lee, and Kristina Toutanova. Bert: Pre-training of deep bidirectional transformers for language understanding. *arXiv preprint arXiv:1810.04805*, 2018.
- [11] Alexey Dosovitskiy, Lucas Beyer, Alexander Kolesnikov, Dirk Weissenborn, Xiaohua Zhai, Thomas Unterthiner, Mostafa Dehghani, Matthias Minderer, Georg Heigold, Sylvain Gelly, et al. An image is worth 16x16 words: Transformers for image recognition at scale. *arXiv preprint arXiv:2010.11929*, 2020.
- [12] John Duchi, Elad Hazan, and Yoram Singer. Adaptive subgradient methods for online learning and stochastic optimization. *Journal of machine learning research*, 12(7), 2011.
- [13] Vladimir Feinberg, Xinyi Chen, Y Jennifer Sun, Rohan Anil, and Elad Hazan. Sketchy: Memory-efficient adaptive regularization with frequent directions. *Advances in Neural Information Processing Systems*, 36, 2024.

- [14] Xuefeng Gao, Mert Gürbüzbalaban, and Lingjiong Zhu. Global convergence of stochastic gradient hamiltonian monte carlo for nonconvex stochastic optimization: Nonasymptotic performance bounds and momentum-based acceleration. *Operations Research*, 70(5):2931–2947, 2022.
- [15] Mary Gooneratne, Khe Chai Sim, Petr Zadrazil, Andreas Kabel, Françoise Beaufays, and Giovanni Motta. Low-rank gradient approximation for memory-efficient on-device training of deep neural network. In *ICASSP 2020-2020 IEEE International Conference on Acoustics, Speech and Signal Processing (ICASSP)*, pages 3017–3021. IEEE, 2020.
- [16] Kaiming He, Xiangyu Zhang, Shaoqing Ren, and Jian Sun. Deep residual learning for image recognition. In *Proceedings of the IEEE conference on computer vision and pattern recognition*, pages 770–778, 2016.
- [17] Diederik P Kingma and Jimmy Ba. Adam: A method for stochastic optimization. *arXiv preprint arXiv:1412.6980*, 2014.
- [18] Jakub Konečný, H Brendan McMahan, Daniel Ramage, and Peter Richtárik. Federated optimization: Distributed machine learning for on-device intelligence. *arXiv preprint arXiv:1610.02527*, 2016.
- [19] Daniel D Lee and H Sebastian Seung. Learning the parts of objects by non-negative matrix factorization. *nature*, 401(6755):788–791, 1999.
- [20] Bingrui Li, Jianfei Chen, and Jun Zhu. Memory efficient optimizers with 4-bit states. *Advances in Neural Information Processing Systems*, 36, 2024.
- [21] Tian Li, Anit Kumar Sahu, Ameet Talwalkar, and Virginia Smith. Federated learning: Challenges, methods, and future directions. *IEEE signal processing magazine*, 37(3):50–60, 2020.
- [22] Bo Liu, Lemeng Wu, Lizhang Chen, Kaizhao Liang, Jiaxu Zhu, Chen Liang, Raghuraman Krishnamoorthi, and Qiang Liu. Communication efficient distributed training with distributed lion. *arXiv preprint arXiv:2404.00438*, 2024.
- [23] Hong Liu, Zhiyuan Li, David Hall, Percy Liang, and Tengyu Ma. Sophia: A scalable stochastic second-order optimizer for language model pre-training. *arXiv preprint arXiv:2305.14342*, 2023.
- [24] Ilya Loshchilov and Frank Hutter. Decoupled weight decay regularization. *arXiv preprint arXiv:1711.05101*, 2017.
- [25] Yang Luo, Xiaozhe Ren, Zangwei Zheng, Zhuo Jiang, Xin Jiang, and Yang You. Came: Confidence-guided adaptive memory efficient optimization. *arXiv preprint arXiv:2307.02047*, 2023.
- [26] Chris J Maddison, Daniel Paulin, Yee Whye Teh, Brendan O’Donoghue, and Arnaud Doucet. Hamiltonian descent methods. *arXiv preprint arXiv:1809.05042*, 2018.
- [27] Mohammad Mozaffari, Sikan Li, Zhao Zhang, and Maryam Mehri Dehnavi. Mkor: Momentum-enabled kronecker-factor-based optimizer using rank-1 updates. *Advances in Neural Information Processing Systems*, 36, 2024.

- [28] Namuk Park and Songkuk Kim. How do vision transformers work? *arXiv preprint arXiv:2202.06709*, 2022.
- [29] Sashank J Reddi, Satyen Kale, and Sanjiv Kumar. On the convergence of adam and beyond. *arXiv preprint arXiv:1904.09237*, 2019.
- [30] Noam Shazeer and Mitchell Stern. Adafactor: Adaptive learning rates with sublinear memory cost. In *International Conference on Machine Learning*, pages 4596–4604. PMLR, 2018.
- [31] Umut Şimşekli, Mert Gürbüzbalaban, Thanh Huy Nguyen, Gaël Richard, and Levent Sagun. On the heavy-tailed theory of stochastic gradient descent for deep neural networks. *arXiv preprint arXiv:1912.00018*, 2019.
- [32] Samuel L Smith, Benoit Dherin, David GT Barrett, and Soham De. On the origin of implicit regularization in stochastic gradient descent. *arXiv preprint arXiv:2101.12176*, 2021.
- [33] Christian Szegedy, Vincent Vanhoucke, Sergey Ioffe, Jon Shlens, and Zbigniew Wojna. Rethinking the inception architecture for computer vision. In *Proceedings of the IEEE conference on computer vision and pattern recognition*, pages 2818–2826, 2016.
- [34] Yingjie Tian, Yuqi Zhang, and Haibin Zhang. Recent advances in stochastic gradient descent in deep learning. *Mathematics*, 11(3):682, 2023.
- [35] Tijmen Tieleman. Lecture 6.5-rmsprop: Divide the gradient by a running average of its recent magnitude. *COURSERA: Neural networks for machine learning*, 4(2):26, 2012.
- [36] Ashish Vaswani, Noam Shazeer, Niki Parmar, Jakob Uszkoreit, Llion Jones, Aidan N Gomez, Łukasz Kaiser, and Illia Polosukhin. Attention is all you need. *Advances in neural information processing systems*, 30, 2017.
- [37] Tianyu Wu, Shizhu He, Jingping Liu, Siqi Sun, Kang Liu, Qing-Long Han, and Yang Tang. A brief overview of chatgpt: The history, status quo and potential future development. *IEEE/CAA Journal of Automatica Sinica*, 10(5):1122–1136, 2023.
- [38] Lechao Xiao, Jeffrey Pennington, and Samuel Schoenholz. Disentangling trainability and generalization in deep neural networks. In *International Conference on Machine Learning*, pages 10462–10472. PMLR, 2020.
- [39] Hongyi Zhang, Moustapha Cissé, Yann Dauphin, and David Lopez-Paz. mixup: Beyond empirical risk minimization. *ArXiv*, abs/1710.09412, 2017.
- [40] J. Zhang, Sai Praneeth Karimireddy, Andreas Veit, Seungyeon Kim, Sashank J. Reddi, Surinder Kumar, and Suvrit Sra. Why adam beats sgd for attention models. *ArXiv*, abs/1912.03194, 2019.
- [41] Jingzhao Zhang, Sai Praneeth Karimireddy, Andreas Veit, Seungyeon Kim, Sashank Reddi, Sanjiv Kumar, and Suvrit Sra. Why are adaptive methods good for attention models? *Advances in Neural Information Processing Systems*, 33:15383–15393, 2020.

- [42] Jiawei Zhao, Zhenyu Zhang, Beidi Chen, Zhangyang Wang, Anima Anandkumar, and Yuan-dong Tian. Galore: Memory-efficient llm training by gradient low-rank projection. *arXiv preprint arXiv:2403.03507*, 2024.
- [43] Pan Zhou, Jiashi Feng, Chao Ma, Caiming Xiong, Steven Chu Hong Hoi, et al. Towards theoretically understanding why sgd generalizes better than adam in deep learning. *Advances in Neural Information Processing Systems*, 33:21285–21296, 2020.

A Hamiltonian function analyses

A.1 Factorized first-order cases

Recall our general framework for factorized first-order methods, which is characterized by the following ODE:

$$\begin{aligned}\dot{X} &= -\nabla\phi(\beta\hat{u}\mathbf{1}_n^\top + \nabla f(X)) - \nabla\psi(\beta\mathbf{1}_m\hat{v}^\top + \nabla f(X)) \\ \dot{u} &= \nabla f(X)\mathbf{1}_n/n - \alpha u, & \hat{u} &= u - \nabla f(X)\mathbf{1}_n/n \\ \dot{v} &= \nabla^\top f(X)\mathbf{1}_m/m - \alpha v, & \hat{v} &= v - \nabla^\top f(X)\mathbf{1}_m/m.\end{aligned}$$

For a canonical example with $\phi(X) = \psi(X) = \|X\|_2^2/2$, and hence $\nabla\phi(X) = \nabla\psi(X) = X$. We will show that the following Hamiltonian function:

$$H(X, u, v) = f(X) + \frac{\beta n}{2} \|u\|_2^2 + \frac{\beta m}{2} \|v\|_2^2,$$

monotonically decreases along the ODE trajectory above. Denote $G = \nabla f(X)$, and note that we can explicitly write the derivative of the model parameter:

$$\dot{X} = -\left(\beta u\mathbf{1}_n^\top + G - \frac{\beta}{n}G\mathbf{1}_n\mathbf{1}_n^\top\right) - \left(\beta\mathbf{1}_m v^\top + G - \frac{\beta}{m}\mathbf{1}_m\mathbf{1}_m^\top G\right),$$

then we can shorten the derivative of the function H as:

$$\begin{aligned}\frac{d}{dt}H &= \text{trace}(G^\top \dot{X}) + \frac{\beta}{n}u^\top \dot{u} + \frac{\beta}{m}v^\top \dot{v} \\ &= -\text{trace}\left(G^\top \left(G - \frac{\beta}{n}G\mathbf{1}_n\mathbf{1}_n^\top\right)\right) - \text{trace}\left(G^\top \left(G - \frac{\beta}{m}\mathbf{1}_m\mathbf{1}_m^\top G\right)\right) - \frac{\alpha\beta}{n}\|u\|_2^2 - \frac{\alpha\beta}{m}\|v\|_2^2 \\ &= -2\|G\|_F^2 + \frac{\beta}{n}\|G\mathbf{1}_n\|_2^2 + \frac{\beta}{m}\|G^\top\mathbf{1}_m\|_2^2 - \frac{\alpha\beta}{n}\|u\|_2^2 - \frac{\alpha\beta}{m}\|v\|_2^2,\end{aligned}$$

in which $\|\cdot\|_F$ is the Frobenius norm. Since $\beta \in (0, 1)$, applying C-S inequality, we have:

$$\frac{d}{dt}H \leq -2\|G\|_F^2 + \frac{1}{n}\|G\mathbf{1}_n\|_2^2 + \frac{1}{m}\|G^\top\mathbf{1}_m\|_2^2 \leq 0. \quad \square$$

A.2 Adafactor

Recall the ODE of Adafactor with momentum:

$$\dot{X} = -\frac{M}{\sqrt{rs^\top/1_m^\top r}}, \quad \dot{M} = \nabla f(X) - \alpha M, \quad \dot{r} = (\nabla f(X))^2\mathbf{1}_n - \alpha r, \quad \dot{s} = (\nabla^\top f(X))^2\mathbf{1}_m - \alpha s.$$

We will show that the Hamiltonian function described by:

$$H(X, M, r, s) = f(X) + \underbrace{\frac{1}{2} \sum_{i=1, j=1}^{m, n} \frac{M_{ij}^2 \sqrt{\sum_{i=1}^m r_i}}{\sqrt{r_i s_j}}}_{\Phi(M, r, s)},$$

is monotonically decreasing along the ODE trajectory.

Denote $G = \nabla f(X)$, we have the derivative of H can be expressed by:

$$\frac{d}{dt}H = \text{trace}(G^\top \dot{X}) + \text{trace}\left((\nabla_M \Phi)^\top \dot{M}\right) + (\nabla_r \Phi)^\top \dot{r} + (\nabla_s \Phi)^\top \dot{s}$$

Analyzing each element specifically, we get:

$$\text{trace}(G^\top \dot{X}) = -\text{trace}\left(G^\top \frac{M\sqrt{1_m^\top r}}{\sqrt{rs^\top}}\right),$$

$$\text{trace}\left((\nabla_M \Phi)^\top \dot{M}\right) = \text{trace}\left((G - \alpha M)^\top \frac{M\sqrt{1_m^\top r}}{\sqrt{rs^\top}}\right) = \text{trace}\left(G^\top \frac{M\sqrt{1_m^\top r}}{\sqrt{rs^\top}}\right) - \alpha \text{trace}\left(M^\top \frac{M\sqrt{1_m^\top r}}{\sqrt{rs^\top}}\right),$$

$$(\nabla_r \Phi)^\top \dot{r} = \sum_{i=1}^m (\partial_{r_i} \Phi)(1_n^\top G_i^2 - \alpha r_i) \quad // G_i \text{ is the } i\text{'th row of } G$$

$$= \sum_{i=1}^m \left(\frac{1}{2} \sum_{j=1}^n \frac{M_{ij}^2}{\sqrt{s_j}}\right) \frac{-\sum_{k \neq i} r_k}{2\sqrt{r_i^{3/2}} \sqrt{\sum_i r_i}} (1_n^\top G_i^2 - \alpha r_i)$$

$$\leq \sum_{i=1}^m \left(\frac{\alpha}{4} \sum_{j=1}^n \frac{M_{ij}^2}{\sqrt{s_j}}\right) \frac{\sum_{k \neq i} r_k}{\sqrt{r_i} \sqrt{\sum_i r_i}} \quad // \text{ the multiplication by } 1_n^\top G_i^2 \text{ is } \leq 0$$

$$\leq \sum_{i=1}^m \left(\frac{\alpha}{4} \sum_{j=1}^n \frac{M_{ij}^2}{\sqrt{s_j}}\right) \frac{\sqrt{\sum_i r_i}}{\sqrt{r_i}} \quad // \sum_{k \neq i} r_k \leq \sum_i r_i$$

$$= \sum_{i=1}^m \left(\frac{\alpha}{4} \sum_{j=1}^n \frac{M_{ij}^2 \sqrt{\sum_i r_i}}{\sqrt{r_i s_j}}\right)$$

$$= \frac{\alpha}{4} \text{trace}\left(M^\top \frac{M\sqrt{1_m^\top r}}{\sqrt{rs^\top}}\right),$$

$$(\nabla_s \Phi)^\top \dot{s} = \sum_{j=1}^n (\partial_{s_j} \Phi)(1_m^\top G_{:j}^2 - \alpha s_j) \quad // G_{:j} \text{ is the } j\text{'th column of } G$$

$$= \sum_{j=1}^n \left(\frac{1}{2} \sum_{i=1}^m \frac{M_{ij}^2 \sqrt{\sum_i r_i}}{\sqrt{r_i}}\right) \frac{-1}{2\sqrt{s_j^{3/2}}} (1_m^\top G_{:j}^2 - \alpha s_j)$$

$$\leq \sum_{j=1}^n \left(\frac{\alpha}{4} \sum_{i=1}^m \frac{M_{ij}^2 \sqrt{\sum_i r_i}}{\sqrt{r_i s_j}}\right) \quad // \text{ the multiplication by } 1_m^\top G_{:j}^2 \text{ is } \leq 0$$

$$= \frac{\alpha}{4} \text{trace}\left(M^\top \frac{M\sqrt{1_m^\top r}}{\sqrt{rs^\top}}\right)$$

Canceling out similar quantities, we can rewrite the Hamiltonian derivative as follows:

$$\frac{d}{dt}H \leq -\frac{\alpha}{2} \text{trace}\left(M^\top \frac{M\sqrt{1_m^\top r}}{\sqrt{rs^\top}}\right) = -\frac{\alpha}{2} \sum_{i=1}^m \sum_{j=1}^n \frac{M_{ij}^2 \sqrt{\sum_i r_i}}{\sqrt{r_i s_j}} \leq 0. \quad \square$$

A.3 H-Fac

In this part, we will prove that the following ODE trajectory:

$$\begin{aligned}\dot{X} &= -\frac{1}{2} \left(\frac{u \mathbf{1}_n^\top - \nabla f(X) \mathbf{1}_n \mathbf{1}_n^\top / n}{\sqrt{r \mathbf{1}_n^\top}} + \frac{\mathbf{1}_m v^\top - \mathbf{1}_m \mathbf{1}_m^\top \nabla f(X) / m}{\sqrt{\mathbf{1}_m s^\top}} \right) - \frac{\nabla f(X)}{\sqrt{r s^\top / \mathbf{1}_m^\top r}} \\ \dot{u} &= \nabla f(X) \mathbf{1}_n / n - \alpha u \\ \dot{v} &= \nabla^\top f(X) \mathbf{1}_m / m - \alpha v \\ \dot{r} &= (\nabla f(X))^2 \mathbf{1}_n - \alpha r \\ \dot{s} &= (\nabla^\top f(X))^2 \mathbf{1}_m - \alpha s\end{aligned}$$

descends the Hamiltonian function defined by:

$$H(X, u, v, r, s) := f(X) + \underbrace{\frac{n}{4} \sum_{i=1}^m \frac{u_i^2}{\sqrt{r_i}} + \frac{m}{4} \sum_{j=1}^n \frac{v_j^2}{\sqrt{s_j}}}_{\Phi(u, v, r, s)}.$$

Denote $G = \nabla f(X)$, we have:

$$\frac{d}{dt} H = \text{trace}(G^\top \dot{X}) + (\nabla_u \Phi)^\top \dot{u} + (\nabla_v \Phi)^\top \dot{v} + (\nabla_r \Phi)^\top \dot{r} + (\nabla_s \Phi)^\top \dot{s}$$

Similar to the previous part, we can calculate each element specifically as follows:

$$\begin{aligned}\text{trace}(G^\top \dot{X}) &= -\frac{1}{2} \text{trace} \left(G^\top \frac{u \mathbf{1}_n^\top}{\sqrt{r \mathbf{1}_n^\top}} \right) - \frac{1}{2} \text{trace} \left(G^\top \frac{\mathbf{1}_m^\top v}{\sqrt{\mathbf{1}_m s^\top}} \right) \\ &\quad + \text{trace} \left(G^\top \frac{G \mathbf{1}_n \mathbf{1}_n^\top}{2n \sqrt{r \mathbf{1}_n^\top}} \right) + \text{trace} \left(G^\top \frac{\mathbf{1}_m \mathbf{1}_m^\top G}{2m \sqrt{\mathbf{1}_m s^\top}} \right) - \text{trace} \left(G^\top \frac{G \sqrt{\mathbf{1}_m^\top r}}{\sqrt{r s^\top}} \right) \\ (\nabla_u \Phi)^\top \dot{u} &= \frac{n}{2} \frac{u^\top}{\sqrt{r^\top}} (G \mathbf{1}_n / n - \alpha u) = \frac{1}{2} \frac{u^\top}{\sqrt{r^\top}} G \mathbf{1}_n - \frac{n\alpha}{2} \frac{u^\top}{\sqrt{r^\top}} u \\ (\nabla_v \Phi)^\top \dot{v} &= \frac{m}{2} \frac{v^\top}{\sqrt{s^\top}} (G^\top \mathbf{1}_m / m - \alpha v) = \frac{1}{2} \frac{v^\top}{\sqrt{s^\top}} G^\top \mathbf{1}_m - \frac{m\alpha}{2} \frac{v^\top}{\sqrt{s^\top}} v \\ (\nabla_r \Phi)^\top \dot{r} &= \left(-\frac{n}{8} \frac{u^2}{\sqrt{r^{3/2}}} \right)^\top (G^2 \mathbf{1}_n - \alpha r) = \frac{n\alpha}{8} \frac{u^2}{\sqrt{r}} - \left(\frac{n}{8} \frac{u^2}{\sqrt{r^{3/2}}} \right)^\top G^2 \mathbf{1}_n \leq \frac{n\alpha}{8} \frac{u^2}{\sqrt{r}} \\ (\nabla_s \Phi)^\top \dot{s} &= \left(-\frac{m}{8} \frac{v^2}{\sqrt{s^{3/2}}} \right)^\top ((G^2)^\top \mathbf{1}_m - \alpha s) = \frac{m\alpha}{8} \frac{v^2}{\sqrt{s}} - \left(\frac{m}{8} \frac{v^2}{\sqrt{s^{3/2}}} \right)^\top (G^2)^\top \mathbf{1}_m \leq \frac{m\alpha}{8} \frac{v^2}{\sqrt{s}}\end{aligned}$$

Canceling out crossing terms, with a note that:

$$\begin{aligned}\text{trace} \left(G^\top \frac{u \mathbf{1}_n^\top}{\sqrt{r \mathbf{1}_n^\top}} \right) &= \frac{u^\top}{\sqrt{r^\top}} G \mathbf{1}_n, & \text{trace} \left(G^\top \frac{\mathbf{1}_m^\top v}{\sqrt{\mathbf{1}_m s^\top}} \right) &= \frac{v^\top}{\sqrt{s^\top}} G^\top \mathbf{1}_m, \\ \frac{u^\top}{\sqrt{r^\top}} u &= \frac{u^2}{\sqrt{r}}, & \frac{v^\top}{\sqrt{s^\top}} v &= \frac{v^2}{\sqrt{s}},\end{aligned}$$

we can rewrite the Hamiltonian derivative as follows:

$$\begin{aligned} \frac{d}{dt}H &\leq \text{trace} \left(G^\top \frac{G1_n1_n^\top}{2n\sqrt{r1_n^\top}} \right) + \text{trace} \left(G^\top \frac{1_m1_m^\top G}{2m\sqrt{1_ms^\top}} \right) - \text{trace} \left(G^\top \frac{G\sqrt{1_m^\top r}}{\sqrt{rs^\top}} \right) \\ &= \text{trace} \left(\frac{1}{n}(G1_n)^2 \frac{1}{2\sqrt{r^\top}} \right) + \text{trace} \left(\frac{1}{m}(G^T1_m)^2 \frac{1}{2\sqrt{s^\top}} \right) - \text{trace} \left(G^2 \frac{\sqrt{1_m^\top r}}{\sqrt{sr^\top}} \right). \end{aligned}$$

Applying C-S inequality gives us $\frac{1}{n}(G1_n)^2 \leq G^21_n$ and $\frac{1}{m}(G^T1_m)^2 \leq (G^T)^21_m$, therefore:

$$\begin{aligned} \frac{d}{dt}H &\leq \text{trace} \left(G^21_n \frac{1}{2\sqrt{r^\top}} \right) + \text{trace} \left((G^T)^21_m \frac{1}{2\sqrt{s^\top}} \right) - \text{trace} \left(G^2 \frac{\sqrt{1_m^\top r}}{\sqrt{sr^\top}} \right), \\ &= \frac{1}{2} \text{trace} \left[\underbrace{G^2 \left(1_n \frac{1}{\sqrt{r^\top}} + \frac{1}{\sqrt{s}} 1_m^\top - 2 \frac{\sqrt{1_m^\top r}}{\sqrt{sr^\top}} \right)}_Q \right]. \end{aligned}$$

By zero initialization, we note that the moving averages of row sums and column sums are symmetric, in other words, $1_m^\top r$ and $1_n^\top s$ are both represent the moving average of the sum of all squared gradient entries. Denote this quantity by \mathcal{S} , we have $\mathcal{S} = 1_m^\top r = 1_n^\top s \geq (r_i + s_j)/2$ for all i, j , then consider each element of matrix Q :

$$\frac{1}{\sqrt{r_i}} + \frac{1}{\sqrt{s_j}} - 2 \frac{\sqrt{\mathcal{S}}}{\sqrt{r_i s_j}} \leq \frac{1}{\sqrt{r_i}} + \frac{1}{\sqrt{s_j}} - \frac{\sqrt{2(r_i + s_j)}}{\sqrt{r_i s_j}} \leq 0,$$

by C-S inequality. Therefore Q is a negative matrix, and as a result, $\frac{d}{dt}H(x_t, u_t, v_t, r_t, s_t) \leq 0$. \square

B Factorized Lion optimizer

Recently, a new optimization named Lion (Evolved Sign Momentum) [6] was discovered by an evolutionary search algorithm applied to a symbolically represented program space. Lion has been shown to achieve at least comparable performance to AdamW on a wide range of tasks while reducing memory cost and training time. Notably, Lion can be formulated as an iterative update procedure:

$$\begin{aligned} M_t &= \beta_2 M_{t-1} + (1 - \beta_2) \nabla f(X_{t-1}) \\ X_t &= X_{t-1} - \eta_t (\text{sign}(\beta_1 M_{t-1} + (1 - \beta_1) \nabla f(X_{t-1})) + \lambda X_{t-1}) \end{aligned} \quad // \text{ Lion}$$

We can see that when $\beta_2 = \beta_1$, Lion will resemble *signSGD* with momentum [2]. However, Lion used a double- β scheme with default values $\beta_1 = 0.9, \beta_2 = 0.99$. Intuitively, this allows Lion to remember longer the gradient history accumulated by the momentum, meanwhile assign a higher weight to the current gradient. Comprehensive experimental results show that Lion converges faster and usually generalizes better than AdamW, but with greater memory efficiency as it only keeps track of the momentum.

Algorithm 4 **Lionfactor** for matrix parameter, with factored first-order moments.

Inputs: double-moment coefficients $\beta_1 = 0.9, \beta_2 = 0.99$, and regularization constant λ

Initialization: weight parameters $X_0 \in \mathbb{R}^{m \times n}$, initial moment factors $u_0, v_0 \leftarrow 0$

for $t = 1$ to T **do**

$$G_t = \nabla f_t(X_{t-1})$$

update model parrameters

$$\hat{u}_t = \beta_1 u_{t-1} + (1 - \beta_1) G_t \mathbf{1}_n / n - G_t \mathbf{1}_n / n$$

$$\hat{v}_t = \beta_1 v_{t-1} + (1 - \beta_1) G_t^\top \mathbf{1}_m / m - G_t^\top \mathbf{1}_m / m$$

$$X_t = X_{t-1} - \eta_t \left(\text{sign} \left(\hat{u}_t \mathbf{1}_n^\top + G_t \right) + \text{sign} \left(\mathbf{1}_m \hat{v}_t^\top + G_t \right) + \lambda X_{t-1} \right)$$

update exponential moment averages

$$u_t = \beta_2 u_{t-1} + (1 - \beta_2) G_t \mathbf{1}_n / n$$

$$v_t = \beta_2 v_{t-1} + (1 - \beta_2) G_t^\top \mathbf{1}_m / m$$

end for

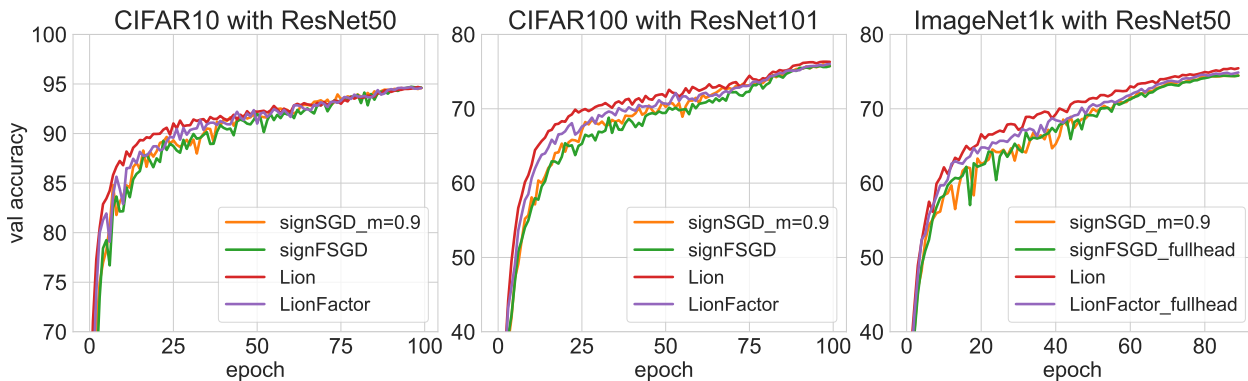


Figure 4: Performance of sign-based optimizers on ResNet architectures. “fullhead” means the version using full momentum for the MLP head layer.

We can similarly apply the double- β scheme to our *signFGSD*, and obtain a new algorithm that we call **LionFactor** 4. We conducted several experiments to evaluate the performance of LionFactor on ResNet models. The results are shown in Figure 4. Interestingly, LionFactor performs significantly better than *signFSGD*, even *signSGD* with momentum, in terms of both convergence rate and accuracy. Although LionFactor still shares the same drawbacks with *signFSGD* when applied to models such as ViTs, it makes a lot of sense to explore more efficient algorithms to factorize the momentum in Lion optimizer. We leave it for future work.

C Pseudocode for Adam and a variant

Algorithm 5 AdamW

Inputs: moment coefficients β_1, β_2 , weight decay constant λ , and smoothing term ϵ .

Initialization: weight parameter $X_0 \in \mathbb{R}^{m \times n}$, initial moments $M_0, V_0 \leftarrow 0$

for $t = 1$ to T **do**

$$G_t = \nabla f_t(X_{t-1})$$

$$M_t = \hat{\beta}_{1t} M_{t-1} + (1 - \hat{\beta}_{1t}) G_t$$

$$V_t = \hat{\beta}_{2t} V_{t-1} + (1 - \hat{\beta}_{2t}) G_t^2$$

$$X_t = X_{t-1} - \eta_t (M_t / (\sqrt{V_t} + \epsilon) + \lambda X_{t-1})$$

end for

Algorithm 6 AdamW variant

Inputs: moment coefficients β_1, β_2 , weight decay constant λ , and smoothing term ϵ .

Initialization: weight parameter $X_0 \in \mathbb{R}^{m \times n}$, initial moments $M_0, V_0 \leftarrow 0$

for $t = 1$ to T **do**

$$G_t = \nabla f_t(X_{t-1})$$

$$V_t = \hat{\beta}_{2t} V_{t-1} + (1 - \hat{\beta}_{2t}) G_t^2$$

$$M_t = \hat{\beta}_{1t} M_{t-1} + (1 - \hat{\beta}_{1t}) G_t / (\sqrt{V_t} + \epsilon)$$

$$X_t = X_{t-1} - \eta_t (M_t + \lambda X_{t-1})$$

end for

We reproduce the pseudocode for the Adam optimizer and its variant. Basically, Adam adopts exponential moving averages to accumulate the first (M_t) and second-order momentum (V_t) through training steps, and then uses the signal-to-noise ratio $M_t/\sqrt{V_t}$ to update the model parameters. While the variant at each iteration, will utilize the second-moment estimator to normalize the current gradient, then exponentially accumulate this normalized value for updating parameters. Our *H-Fac* shares the same principles as this variant.